doi:10.3772/j.issn.1006-6748.2019.02.010

Dynamic analysis of double-layer and pre-stressed multi-limb six-axis force sensor①

Wang Zhijun(王志军)②[*,***], He Jing[**], Cui Bingyan[*,***], Li Zhanxian[*,***]
([*] College of Mechanical Engineering, North China University of Science and Technology, Tangshan 063210, P. R. China)
([**] Tangshan Polytechnic College, Tangshan 063299, P. R. China)
([***] Hebei Province Research Institute of Industrial Robot Industry Technology, Tangshan 063210, P. R. China)

Abstract

In order to adapt to the specific task, the six-axis dynamic contact force between end-effectors of intelligent robots and working condition needs to be perceived. Therefore, the dynamic property of six-axis force sensor which is installed on the end-effectors of intelligent robots will have influence on the veracity of detection and judgment to working environment contact force by intelligent robots directly. In this paper, dynamic analysis to double-layer and pre-stressed multi-limb six-axis force sensor is conducted. First, the structure of the sensor is introduced, and the limb number is confirmed by introducing the related definitions of convex analysis. Then, based on vibration of multiple-degree-of-freedom system, a mechanical vibration simplified model of double-layer and pre-stressed multiple limb six-axis force sensor is set up. After that, movement differential equations of sensor and the response of analytical expression are deduced, and the movement differential equations is solved. Finally, taking the double-layer and pre-stressed seven limb six-axis force sensor as an example, numerical calculation and simulation of deriving result is conducted, which verify the correctness and feasibility of the theoretical analysis.

Key words: six-axis force sensor, multi-limb, pre-stressed, mechanical vibration, dynamic analysis

0 Introduction

With continuous development of computer technology, the intelligent level and interaction ability of robots are increasing rapidly. In the field of the robot, intelligent sensor makes robots have the function similar to the five sense organs and brain of humans. So, an intelligent robot system is the sensor integration[1,2]. Because it can realize the force perception of robot in working condition, force sensor becomes very important. When robot motion is in three-dimensional space the load upon anywhere of robot actually contains three directions of force and three directions of moment. Therefore, six-axis force sensor which can detect six force components simultaneously is needed on the robot's wrist contacting with the working condition to make robot have full force information of working condition.

In 1983, the Stewart platform parallel structure was used in designing six-axis force sensor firstly by Gaillet and Reboulet[3]. Since then, this type of sensors has received more attention of many scholars in the world. With its inherent advantages like high stiffness, stable structure, high carrying capacity, no error accumulation and easiness to solve inverse kinematics[4], the Stewart parallel structure has become a successful implementation of six-axis force sensor structure. In actual detection of the six dimensional force sensor at present, 6-dimensional dynamic forces need to be measured in more and more situations. Veracity of measurement and real-time performance of control are influenced by merits of sensor's performance dynamic. Six-axis force sensor is demanded to reflect the variation of measured contact force accurately and rapidly in many dynamic and quasi-static fields. Therefore, the dynamic performance of six-axis force sensor becomes very important. Fujii[5] contrasted and discussed multiple force sensors' dynamic calibration methods, and put forward a levitated-mass method to realize accurate

① Supported by the National Natural Science Foundation of China (No. 51505124), the Natural Science Foundation of Hebei Province (No. E2016209312) and the Foster Fund Projects of North China University of Science and Technology (No. JP201505).
② To whom correspondence should be addressed. E-mail: zjwang@ncst.edu.cn
Received on June 5, 2018

measurement of inertia force. Kim et al. [6,7] developed a 6-axis force/moment sensor to use it as an intelligent robot's gripper for safely grasping an unknown object and accurately perceiving the position of the object in the grippers. Li et al. [8,9] presented a novel parallel spoke piezoelectric 6-DOF heavy force/torque sensor by using adjustable load sharing device, and discussed the static and dynamic calibration experiments for fabricated piezoelectric force/torque sensor. Hirose et al. [10] proposed the dynamic motion analysis method of ski turns using the inertial and force sensors. Yuan et al[11] developed and evaluated of a six-axis force/moment sensor used under humanoid robot foot, and carried out a characteristic test of the developed sensor. Sun et al. [12] designed and optimized a novel six-axis force/torque sensor based on strain gauges for space robot developed, which has a rather good performance in sensitivity, nonlinearity, repeatability, stability, hysteresis, and accuracy. Chen et al. [13], focusing on the following special requirements of space application, large measurement range, high reliability and high precision, designed a six-axis force/torque sensor, which could be used as a component for the large manipulator in the space station. Zhao et al. [14] demonstrated a kind of six-axis force sensor based on 6-UPUR parallel mechanism with flexible joints, which has large measurement range and high accuracy.

The measuring limbs of Stewart platform parallel structure are tow-force bars in theory. No stress coupled 6-dimensional forces measure is realizable among sensitive elements. But in the actual measurement, because there is friction on spherical pair after pre-tightening, strict linear relationship between 6-axis forces with action on the force sensor and axial force of measuring limbs are no longer presented, thereby it leads to a certain measurement error and restrains application of this kind of sensor in practice[15]. Sensor of double-layer and pre-stressed multiple limb six-axis force both keeps the advantage of Stewart platform parallel structure and greatly overcomes the main drawback of the described earlier. A preloaded platform of double-layer and pre-stressed multiple limb six-axis force sensor is added between top and bottom platforms, and two ends of the measuring limb are connected with the platforms using the cone-shaped spherical pairs instead of the traditional spherical pairs. Thus the clearance of spherical pair is eliminated, the overall stiffness of sensor is improved and friction torque of traditional spherical pair is diminished significantly.

In this paper, the simplified model of mechanical vibration of double-layer and pre-stressed multiple limb six-axis force sensor is set up firstly based on vibration of multiple-degree-of-freedom system. Then, the movement differential equations of sensor and the response of analytical expression are deduced, and the movement differential equations are solved. Finally, taking the double-layer and pre-stressed seven limb six-axis force sensor as an example, numerical calculation and simulation of deriving result is conducted, which verify the correctness and feasibility of the theoretical analysis.

1 Double-layer and pre-stressed multi-limb six-axis force sensor

1.1 Structure of the double-layer and pre-stressed multi-limb six-axis force sensor

Fig. 1 is the schematic diagram of double-layer and pre-stressed multiple limb six-axis force sensor. It is composed of a pre-stressed platform, a measuring platform, measuring limbs and a base platform. The measuring limbs composed of integrated one-dimensional force sensors are connected with platforms by cone-shaped spherical pair instead of traditional spherical pair and divided into two layers to distribute on both sides of the up and down measuring platform. The contact area of two types spherical pairs is compared in Fig. 2. o is the center of spherical pair, curves c_1 and c_2 are projections of contact surface in limb plane, f represents the direction of the affordable force of limb. From Fig. 2, in the case of ensuring the contact strength, the cone-shaped spherical pair can realize a small contact area thus efficaciously reduce the friction moment on contact surface of spherical pair. Besides, the cone-shaped spherical pair only makes limbs suffer from stress, thereby, zero passage is non-existent, the impact of force contact with spherical contact surface is eliminated, and the integral rigidity is improved.

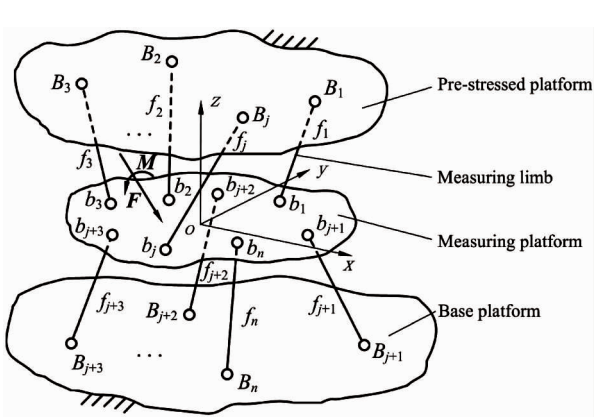

Fig. 1 Schematic diagram of the double-layer and pre-stressed multiple limb six-axis force sensor

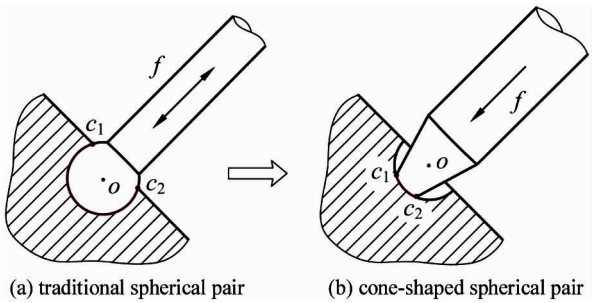

Fig. 2 Comparison of the contact area of spherical pair

Before measuring, making each measuring limb have a certain initial pre-stressed force by means of compressing pre-stressed platform and measuring platform to ensure that measuring limbs are always pressed in the process of measurement. When measuring, external force is applied to measuring platform, axis force will be measured by measuring limbs that are distributed on both sides of the up and down of measuring platform. Then 6-dimensional external force will be obtained by static equilibrium. Putting measuring limbs to distribute on both sides of the up and down of measuring platform and take some advantages like stable pre-stressed way, high rigidity and large over turning moment can be supported.

1.2 Determination of measuring limb count

The unilateral constraint of cone-shaped spherical pairs is similar to the frictionless point contact. So if the sensor wants to resist any external force, it must be in the state of force-closure[16-18]. Moreover, the pattern of force-closure is determined by the number of the sensor's measuring limbs. For the double-layer pre-stressed multiple limb six-axis force sensor, upper and lower bounds for the number of measuring limbs required for a force-closure constraint can be obtained by using two classical theorems in convex analysis.

Theorem 1 (Caratheodory). If a set $\boldsymbol{X} = \{v_1, v_2, \cdots, v_k\}$ positively spans $\boldsymbol{R}^p$, then $k \geqslant p + 1$.

Theorem 2 (Steinitz). If $S \subset R^p$ and $q \in \text{int}(\text{co}\ \boldsymbol{S})$, then there exists $\boldsymbol{X} = \{v_1, v_2, \cdots, v_k\} \subset \boldsymbol{S}$ such that $q \in \text{int}(\text{co}\ \boldsymbol{X})$ and $k \leqslant 2p$. Let co $\boldsymbol{S}$ denote the convex hull of set $\boldsymbol{S}$, int(co $\boldsymbol{S}$) denote the interior of the convex hull.

Theorem 1 and Theorem 2 allow us to bound the number of contacts required for a force-closure grasp using frictionless point contacts. Caratheodory's theorem implies that if a rigid body can be restricted with a force-closure state, then it must have at least $p + 1$ unilateral contacts. And Steinitz's theorem places an upper bound on the minimal number of unilateral contacts which are needed. For a rigid body in three-dimensional space, the applied external force is six-dimensional (three-dimensional force and three-dimensional torque), so at least seven and at most twelve measuring limbs will be available in order to restrict the measuring platform in the state of static balance.

2 Vibration mechanics equation of single limb

Double-layer and pre-stressed multiple limb six-axis force sensor is a complex multiple parallel limbs system with the characteristic of that every limb is single-degree-of-freedom system in same structure. As the basis of overall vibration mechanics analysis, the vibration mechanics model of single measuring limb should be built firstly. A single measuring limb can be regarded as an idealized element in ideal, and a single-degree-of-freedom system is composed of mass piece, damper and spring. The simplified model of vibration mechanics is shown as Fig. 3.

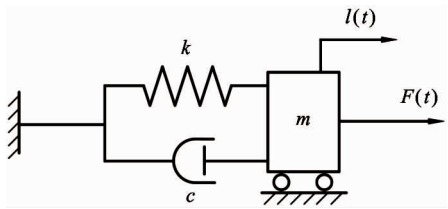

Fig. 3 Vibration mechanics model of a single measuring limb

The movement differential equation of single measuring limb is built as

$$m\ddot{l}(t) + c\dot{l}(t) + kl(t) = f(t) \tag{1}$$

where k, c, m, $l(t)$ and $f(t)$ are equivalent stiffness, equivalent damping, equivalent mass, axial direction displacement and limb axial direction of sensor measuring limb.

From Eq. (1), put all measuring limbs together and rewrite them as the matrix equation:

$$[\boldsymbol{m}]\ddot{\boldsymbol{l}}(t) + [\boldsymbol{c}]\dot{\boldsymbol{l}}(t) + [\boldsymbol{k}]\boldsymbol{l}(t) = \boldsymbol{f}(t) \tag{2}$$

where $\boldsymbol{l}(t) = [l_1(t)\ \ l_2(t)\ \ \cdots\ \ l_n(t)]^{\mathrm{T}}$, $[\boldsymbol{m}] = \text{diag}(m_1, m_2, \cdots, m_n)$, $[\boldsymbol{c}] = \text{diag}(c_1, c_2, \cdots, c_n)$, $[\boldsymbol{k}] = \text{diag}(k_1, k_2, \cdots, k_n)$, $\boldsymbol{f}(t) = [f_1(t)\ \ f_2(t)\ \ \cdots\ \ f_n(t)]^{\mathrm{T}}$, n is the number of measuring limbs.

Under the initial circumstances of no external forces, the system is preloading. There is only pre-stressed force on measuring limb. When $t = 0$, the initial conditions of initial force, initial displacement and initial velocity in Eq. (2) are expressed as

$$\boldsymbol{f}(t) \mid t = 0 = \boldsymbol{f}_{\mathrm{P}} \tag{3}$$

$$\boldsymbol{l}(t)\mid_{t=0} = \boldsymbol{l}_0 = \mathrm{diag}\left(\frac{1}{k_1},\frac{1}{k_2},\cdots,\frac{1}{k_n}\right)\boldsymbol{f}_{\mathrm{P}} \quad (4)$$

$$\dot{\boldsymbol{l}}(t)\mid_{t=0} = \ddot{\boldsymbol{l}}(t)\mid_{t=0} = \boldsymbol{0} \quad (5)$$

3 Vibration mechanics equation of the force sensor

Then make the pre-stressed multiple limb six-axis force sensor as the object of study and build the vibration mechanics equation of system. Assuming that measuring platform is rigid body, when generalized 6-dimensional external force $F(t)$ is applied on measuring platform the generalized coordinates $\boldsymbol{q}(t) = [q_1 \quad q_2 \quad q_3 \quad q_4 \quad q_5 \quad q_6]^{\mathrm{T}}$ is used to describe the motion of it. $\boldsymbol{x}(t) = [q_1 \quad q_2 \quad q_3]^{\mathrm{T}}$ is 3-dimensional moving coordinates of measuring platform, and $\boldsymbol{\theta}(t) = [q_4 \quad q_5 \quad q_6]^{\mathrm{T}}$ is 3-dimensional rotational coordinates of measuring platform. Choosing $q(t)$ as generalized coordinates of the system can eliminate coupling among generalized coordinates, and solve movement differential equation easily.

As shown in Fig. 4, the simplified vibration mechanics model of multiple limb six-axis force sensor is built. This model is combined with multiple spatial single-degree-of-freedom system and a mass piece M. Each limb is single-degree-of-freedom system with damped spring mass. The reference coordinate system of overall system is o-xyz.

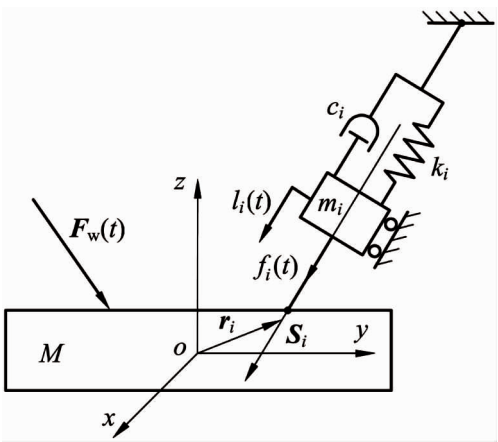

Fig. 4 Vibration mechanics model of the multiple limb six-axis force sensor

The relationship between liner-displacement of measuring limb and generalized coordinates $q(t)$ will be built. For initial state $t = 0$, each limb's liner-displacement caused by pre-stressed force is $l_{i0}(i = 1,2,\cdots,n)$. Then the liner-displacement of limb i is expressed as

$$\begin{aligned} l_i(t) &= \boldsymbol{S}_i[\boldsymbol{x}(t) + \boldsymbol{\theta}(t) \times \boldsymbol{r}_i] + l_{i0} \\ &= [\boldsymbol{S}_i^{\mathrm{T}} \quad (\boldsymbol{r}_i \times \boldsymbol{S}_i)^{\mathrm{T}}]\begin{bmatrix}\boldsymbol{x}(t)\\ \boldsymbol{\theta}(t)\end{bmatrix} + \frac{f_{\mathrm{P}i}}{k_i} \end{aligned} \quad (6)$$

where $\boldsymbol{S}_i$ is the direction vector of limb i axis, $\boldsymbol{r}_i$ is the position vector of a point on limb i axis.

Putting all limbs together and the liner-displacement of limbs can be rewritten in the form of matrix as

$$\boldsymbol{l}(t) = \boldsymbol{G}^{\mathrm{T}}\boldsymbol{q}(t) + \left[\frac{1}{\boldsymbol{k}}\right]\boldsymbol{f}_{\mathrm{P}} \quad (7)$$

where

$$\left[\frac{1}{\boldsymbol{k}}\right] = \mathrm{diag}\left(\frac{1}{k_1} \quad \frac{1}{k_2} \quad \cdots \quad \frac{1}{k_n}\right) \quad (8)$$

$$\boldsymbol{G} = \begin{bmatrix} \boldsymbol{S}_1 & \boldsymbol{S}_2 & \cdots & \boldsymbol{S}_n \\ \boldsymbol{r}_1 \times \boldsymbol{S}_1 & \boldsymbol{r}_2 \times \boldsymbol{S}_2 & \cdots & \boldsymbol{r}_n \times \boldsymbol{S}_n \end{bmatrix} \quad (9)$$

Supposing that Eq. (9) does not change with time, which means $\frac{\partial \boldsymbol{G}^{\mathrm{T}}}{\partial t} = 0$. The derivative of Eq. (9) can be expressed as

$$\dot{\boldsymbol{l}}(t) = \boldsymbol{G}^{\mathrm{T}}\dot{\boldsymbol{q}}(t) \quad (10)$$

$$\ddot{\boldsymbol{l}}(t) = \boldsymbol{G}^{\mathrm{T}}\ddot{\boldsymbol{q}}(t) \quad (11)$$

Substituting Eqs(7), (10) and (11) into Eq. (2), Eq. (12) will be got:

$$[\boldsymbol{m}]\boldsymbol{G}^{\mathrm{T}}\ddot{\boldsymbol{q}}(t) + [\boldsymbol{c}]\boldsymbol{G}^{\mathrm{T}}\dot{\boldsymbol{q}}(t) + [\boldsymbol{k}]\boldsymbol{G}^{\mathrm{T}}\boldsymbol{q}(t) + \boldsymbol{f}_{\mathrm{P}} = \boldsymbol{f}(t) \quad (12)$$

Then taking mass piece $\boldsymbol{M}$ of measuring platform into account, the differential equation can be obtained as

$$[\boldsymbol{M}_0]\ddot{\boldsymbol{q}}(t) + \boldsymbol{G} \cdot \boldsymbol{f}(t) = \boldsymbol{F}_{\mathrm{w}}(t) \quad (13)$$

where $[\boldsymbol{M}_0] = \mathrm{diag}(M_0, M_0, M_0, I_{0x}, I_{0y}, I_{0z})$ is the matrix of measuring platform's mass. M_0 is the mass of measuring platform, and I_{0x}, I_{0y}, I_{0z} are rotational inertia of measuring platform rotating about coordinate axis.

When no external forces and torques are applied on the platform of the sensor, that is $\boldsymbol{G} \cdot \boldsymbol{f}_{\mathrm{P}} = \boldsymbol{0}$, Substituting Eq. (12) into Eq. (13) and simplifying, the following equation can be obtained

$$[\boldsymbol{M}]\ddot{\boldsymbol{q}}(t) + [\boldsymbol{C}]\dot{\boldsymbol{q}}(t) + [\boldsymbol{K}]\boldsymbol{q}(t) = \boldsymbol{F}_{\mathrm{w}}(t) \quad (14)$$

where $[\boldsymbol{M}] = [\boldsymbol{M}_0] + \boldsymbol{G}[\boldsymbol{m}]\boldsymbol{G}^{\mathrm{T}}$ is the matrix of systematic total mass, $[\boldsymbol{C}] = \boldsymbol{G}[\boldsymbol{c}]\boldsymbol{G}^{\mathrm{T}}$ is the matrix of systematic total damping, $[\boldsymbol{K}] = \boldsymbol{G}[\boldsymbol{k}]\boldsymbol{G}^{\mathrm{T}}$ is the matrix of systematic total stiffness.

Eq. (14) is the movement differential equation of the multiple-degree-of-freedom system. From Eq. (14), there is no relationship between sensor system responses $q(t)$ and initial pre-stressed force $\boldsymbol{f}_{\mathrm{P}}$. System response $q(t)$ is obtained by solving Eq. (14). Then substituting $q(t)$ into Eq. (12), the force response of measuring limbs can be obtained as

$$\boldsymbol{f}(t) = [\boldsymbol{m}]\boldsymbol{G}^{\mathrm{T}}\ddot{\boldsymbol{q}}(t) + [\boldsymbol{c}]\boldsymbol{G}^{\mathrm{T}}\dot{\boldsymbol{q}}(t) + [\boldsymbol{k}]\boldsymbol{G}^{\mathrm{T}}\boldsymbol{q}(t) + \boldsymbol{f}_{\mathrm{P}} \tag{15}$$

Each limb's force response $\boldsymbol{f}(t)$ can be obtained by solving Eq. (15).

4 Solving of the movement differential equation

4.1 Solving of the non-damping free vibration movement differential equation

Under the circumstance of non-damping free vibration, system movement differential of Eq. (14) can be rewritten as

$$[\boldsymbol{M}]\ddot{\boldsymbol{q}}(t) + [\boldsymbol{K}]\boldsymbol{q}(t) = 0 \tag{16}$$

Eq. (16) can be extended as

$$\sum_{j=1}^{6} m_{ij}\ddot{q}_j(t) + \sum_{j=1}^{6} k_{ij}q_j(t) = 0 \quad (i = 1,2,\cdots,n) \tag{17}$$

where m_{ij} and k_{ij} are line i column j element of systematic mass matrix and stiffness matrix respectively.

Adopt the way of synchronization solution[19] to solve Eq. (17). Supposing that

$$q_j(t) = u_j f(t) \quad (j = 1,2,\cdots,6) \tag{18}$$

where $u_j (j = 1,2,\cdots,6)$ is a constant, and $f(t)$ is a function only related to time.

The homogeneous algebraic equation about $\boldsymbol{u} = (u_1 \quad u_2 \quad \cdots \quad u_6)$ is expressed as follows

$$[\boldsymbol{K}]\boldsymbol{u} - \omega^2[\boldsymbol{M}]\boldsymbol{u} = 0 \tag{19}$$

where ω is frequency of simple harmonic motion.

The necessary sufficient condition that makes the equation have untrivial solution is the coefficient determinant equals to zero. That is to say

$$\Delta(\omega^2) = |[\boldsymbol{K}] - \omega^2[\boldsymbol{M}]| = 0 \tag{20}$$

Eq. (20) is the systematic frequency equation. Each order systematic inherent frequency $\omega_r (r = 1,2,\cdots,6)$ can be obtained by solving the equation.

Substituting r order inherent frequency ω_r into Eq. (19), then solution $\boldsymbol{u}_r$ of response can be obtained. Systematic generalized coordinates' response under r order inherent frequency is

$$\boldsymbol{q}_r(t) = A\boldsymbol{u}_r\cos(\omega_r t - \varphi) \quad (r = 1,2,\cdots,6) \tag{21}$$

where ω_r and $\boldsymbol{u}_r$ are decided by the system parameter, A and φ are decided by the initial conditions.

4.2 Solving of the general response of vibration movement differential equation

Using the method of vibration system modal analysis, the general response of differential equation of the force sensor can be solved as follows. Firstly, r order inherent frequency ω_r and corresponding modal vector $\boldsymbol{u}_r$ can be obtained from Eq. (20). Systematic modal matrix can be expressed as follows.

$$[\boldsymbol{u}] = [\boldsymbol{u}_1 \quad \boldsymbol{u}_2 \quad \cdots \quad \boldsymbol{u}_6] \tag{22}$$

Substituting natural coordinates $\boldsymbol{\eta}(t)$ for generalized coordinates $\boldsymbol{q}(t)$ of movement differential equation, moreover the relationship between $\boldsymbol{\eta}(t)$ and $\boldsymbol{q}(t)$ can be expressed as follows

$$\boldsymbol{q}(t) = [\boldsymbol{u}]\boldsymbol{\eta}(t) \tag{23}$$

Because the modal matrix is constant matrix, thus

$$\dot{\boldsymbol{q}}(t) = [\boldsymbol{u}]\dot{\boldsymbol{\eta}}(t), \quad \ddot{\boldsymbol{q}}(t) = [\boldsymbol{u}]\ddot{\boldsymbol{\eta}}(t) \tag{24}$$

Substituting Eqs (23) and (24) into Eq. (14), and premultiplication $[\boldsymbol{u}]^{\mathrm{T}}$, Eq. (25) is obtained

$$[\boldsymbol{u}]^{\mathrm{T}}[\boldsymbol{M}][\boldsymbol{u}]\ddot{\boldsymbol{\eta}}(t) + [\boldsymbol{u}]^{\mathrm{T}}[\boldsymbol{C}][\boldsymbol{u}]\dot{\boldsymbol{\eta}}(t) + [\boldsymbol{u}]^{\mathrm{T}}[\boldsymbol{K}][\boldsymbol{u}]\boldsymbol{\eta}(t) = [\boldsymbol{u}]^{\mathrm{T}}\boldsymbol{F}_w(t) \tag{25}$$

Then making the modal vector orthonormal by orthogonality, and regarding the systematic damping as proportional damping or small damping, Eq. (25) can be simplified as

$$\ddot{\boldsymbol{\eta}}(t) + [2\xi_r\omega_r]\dot{\boldsymbol{\eta}}(t) + [\omega_r^2]\boldsymbol{\eta}(t) = [\boldsymbol{u}]^T F_{\mathrm{w}}(t) \tag{26}$$

where matrixes $[2\xi_r\omega_r]$ and $[\omega_r^2]$ are the diagonal matrix with diagonal elements $2\xi_r\omega_r$ and $\omega_r^2 (r = 1,2,\cdots,6)$. $\xi_r (r = 1,2,\cdots,6)$ is the damping ratio of systematic r order modal.

After the linear transformation of coordinates mentioned above, the movement differential equation of multiple limb six-axis force sensor is expressed as Eq. (26). The equation is decoupled to natural coordinates $\boldsymbol{\eta}(t)$. Therefore, Eq. (26) is the differential equation with six single-degree-of-freedom system in equivalently that can be solved by the way of single-degree-of-freedom system movement differential equation. Eq. (26) can be solved as follows.

$$\boldsymbol{\eta}_r(t) = \frac{1}{\omega_r\sqrt{1-\xi_r^2}}\int_0^t [\boldsymbol{u}_r]^{\mathrm{T}}\boldsymbol{F}_{\mathrm{w}}(\tau)\,\mathrm{e}^{-\xi_r\omega_r(t-\tau)} \sin[\omega_r\sqrt{1-\xi_r^2}(t-\tau)]\,\mathrm{d}\tau \tag{27}$$

When the six-dimensional dynamic external force changes as sine function, that is to say, $F_{\mathrm{w}}(t) = F_0\sin(\omega t)$, substituting it into Eq. (27) and the responses of steady state forced vibration are

$$\boldsymbol{\eta}_r(t) = \frac{[\boldsymbol{u}_r]^{\mathrm{T}}F_0\sin(\omega t - \varphi_r)}{\omega_r^2\sqrt{[1-(\omega/\omega_r)^2]^2 + (2\xi_r\omega/\omega_r)^2}}$$

$$\varphi_r = \mathrm{tg}^{-1}\frac{2\xi_r\omega/\omega_r}{1-(\omega/\omega_r)^2} \quad (r = 1,2,\cdots,6) \tag{28}$$

where F_0 is the amplitude of imposed six-dimensional force, $F_0 = [F_{x0} \quad F_{y0} \quad F_{z0} \quad M_{x0} \quad M_{y0} \quad M_{z0}]^{\mathrm{T}}$.

Substituting Eq. (28) into Eq. (23), the responses of the generalized coordinates can be obtained as

$$\boldsymbol{q}_r(t) = \frac{[\boldsymbol{u}_r][\boldsymbol{u}_r]^{\mathrm{T}} F_0 \sin(\omega t - \varphi_r)}{\omega_r^2 \sqrt{[1-(\omega/\omega_r)^2]^2 + (2\xi_r\omega/\omega_r)^2}} \tag{29}$$

Substituting the solution of movement differential equation from Eq. (29) into Eq. (15), the response of measuring limbs' axis forces with six-dimensional dynamic external force under this modality can be obtained.

Till now, the solving of six-axis force sensor movement differential equation is completed. It can be seen that the mass matrix, damping matrix and stiffness matrix in movement differential equation can be measured on the basis of real condition. In that way, substituting them into Eq. (13), then the theoretical solution of dynamic force applied on the multiple limb six-axis force sensor can be obtained by Eq. (29).

5 Solving and simulation of movement differential equation

According to the theoretical derivation described above, for double-layer and pre-stressed 7-limb six-axis force sensor, the inherent frequency and the response with six-dimensional dynamic force are solved as follows.

Vibration system space modal of double-layer and pre-stressed 7-limb six-axis force sensor are shown in Fig. 5. $b_1 - b_7$ and $B_1 - B_7$ express the position of the centre of sphere in spherical pair of measuring limbs' both ends. $m_1 - m_7$, $k_1 - k_7$, $c_1 - c_7$ and $\boldsymbol{S}_1 - \boldsymbol{S}_7$ are mass, stiffness, damping and axis position vector of seven measuring limbs respectively. The reference coordinate system *o-xyz* of vibration system modal is built on the downside center of middle platform. M is mass piece of measuring platform, whose mass is M_0, and the rotational inertias of measuring platform to coordinate system *o-xyz* on each direction are expressed as I_{0x}、I_{0y}、I_{0z}.

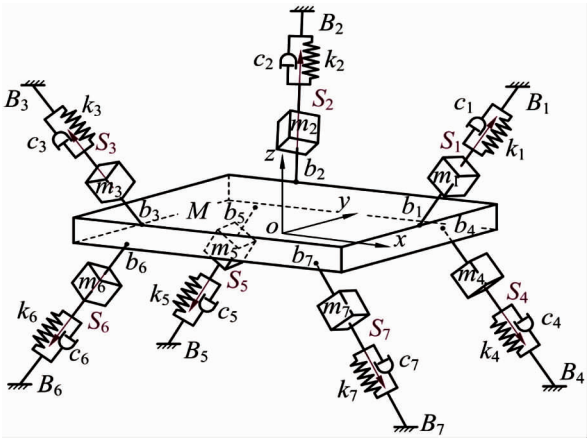

Fig. 5 Vibration system spatial model of the double-layer pre-stressed seven limbs six-axis force sensor

The structure parameters of the double-layer and pre-stressed 7-limb six-axis force sensor are: $r = 25$ mm, $R = 40$ mm, $h = 9$ mm, $l = 31$ mm, $\alpha = \frac{\pi}{4}$, $\beta = \frac{\pi}{6}$. The meanings of symbols are the same as Ref. [20]. The mass and inertia of each part form CAD software are obtained as follows: the mass of measuring platform M_0 is 0.5334 kg. The rotational inertias I_{0x}、I_{0y} are 2.8487×10^{-3} kg · m^2, I_{0z} is 0.6681×10^{-3} kg · m^2. The mass of measuring limb m_i is 1.9322×10^{-2} kg ($i = 1,2,\cdots,7$). And the axial stiffness k_i is 1.12×10^7 N/m ($i = 1,2,\cdots,7$). Substituting the parameters into systemic frequency equation, the theoretical value of the first six order inherent frequency ω_r ($r = 1,2,\cdots,6$) can be obtained. Modal analysis is simulated by ADAMS software, and each order inherent frequency is also obtained. The theoretical values and the simulated values are listed in Table 1. From Table 1, the maximum relative error between theoretical value and simulated value is 12.5%, which demonstrates the correctness of the theoretical analysis. The error is mainly caused by the simplification of the simulation model.

Table 1 Results of the natural frequency of the sensor

6-dimensional force/torque		F_x	F_y	F_z	M_x	M_y	M_z
Inherent frequency (Hz)	Theoretical value	207.9	194.9	305.5	268.4	239.5	322.2
	Simulated value	227.5	219.3	338.5	290.0	259.9	350.4
Relative error (%)		9.4	12.5	10.8	8.0	8.5	8.8

It is provided that the dynamic force $F_z(t) = F_0 \cos\omega t$ is applied on the center of sensor measuring platform, where $F_0 = 200$ is the amplitude of external force, and $\omega = 1000\pi$ Hz is frequency. Expressing the dynamic force $F_w(t) = [0 \quad 0 \quad F_0\cos\omega t \quad 0 \quad 0 \quad 0]^{\mathrm{T}}$ as the 6- dimension force, then assuming the initial condition is $\boldsymbol{q}(0) = \dot{\boldsymbol{q}}(0) = 0$ and pretightening forces of each limb are $f_{\mathrm{P}} = [111 \quad 111 \quad 111 \quad 89 \quad 89 \quad 89]$

N, the steady state response under systemic generalized coordinates can be obtained by substituting them into Eq. (29).

Taking the vertical movement of measuring platform, i. e. generalized coordinate $q_3(t)$ as an example, the response curves of the generalized coordinate $q_3(t)$ and measuring limb axis force $f_1(t)$ are shown as dash line in Fig. 6. The time-varying response curves of sensor middle platform's movement and each measuring limb stress under effect with external force $F_z(t)$ are obtained by ADAMS dynamics simulation. The simulation results are shown as solid line in Fig. 6. Fig. 6(a) shows the time-varying curves of generalized coordinate $q_3(t)$, and Fig. 6(b) shows the time-varying curves of $F_z(t)$ and $f_1(t)$. It shows that the simulation results of the generalized coordinate $q_3(t)$ and the force response $f_1(t)$ are consisitent with the theoretical calculation results.

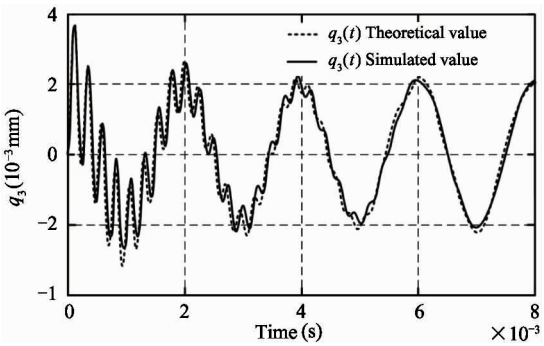

(a) Variation curve of $q_3(t)$ versus time

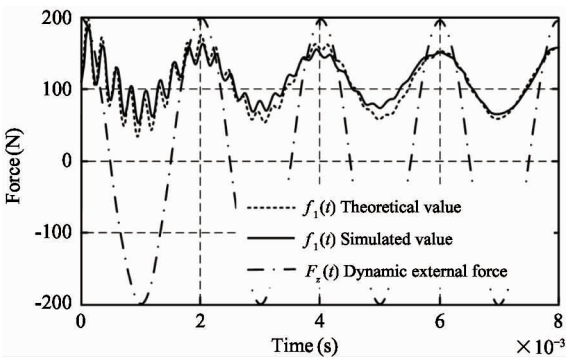

(b) Variation curve of $f_1(t)$ versus time

Fig. 6 Variation curve of theoretical calculation and simulation results

6 Conclusion

This paper conducts the dynamic analysis of a double-layer and pre-stressed multiple limb six-axis force sensor. Firstly, the structure of the double-layer and pre-stressed multiple limb six-axis force sensor is introduced. The number of measuring limb is confirmed according to the related definitions of convex analysis, and at least seven and at most twelve measuring limbs can be available in order to restrict the measuring platform to be staticly balanced. Then, based on the vibration of multiple-degree-of-freedom system, vibration mechanics equation of a single limb is built. Based on this, the vibration mechanics equation of sensor system is deduced, and the solving process of movement differential equation is deduced. Finally, taking the double-layer and pre-stressed seven limbs six-axis force sensor as an example, the numerical solution of inherent frequency and response of applied external force are calculated, and simulation analysis using ADAMS software is carried out. The simulation result is consistent with the numerical calculation which demonstrates the correctness of the theoretical analysis.

References

[1] Xiong Y L. Isotropic of robot force sensor[J]. *Acta Automatic*, 1996, 22: 10-18 (In Chinese)

[2] Palli G, Moriello L, Scarcia U, et al. Development of an optoelectronic 6-axis force/torque sensor for robotic applications[J]. *Sensors and Actuators A: Physical*, 2014, 220: 333-346

[3] Gaillet A, Reboulet C. An isostatic six component force and torque sensor[C]. In: Proceedings of the 13th International Symposium on Industrial Robots, Chicago, USA, 1983. 102-111

[4] Merlet J P. Parallel robots (second edition II) [M]. Berlin: Springer, 2006. 265-266

[5] Fujii Y. Toward dynamic force calibration[J]. *Measurement*, 2009, 42: 1039-1044

[6] Kim G S, Lee H D. Development of a six-axis force/moment sensor and its control system for an intelligent robot's gripper[J]. *Measurement Science and Technology*, 2003, 14: 1265-1274

[7] Kim G S, Shin H J, Yoon J. Development of 6-axis force/moment sensor for a humanoid robot's intelligent foot[J]. *Sensors and Actuators A: Physical*, 2008, 141 (2): 276-281

[8] Li Y J, Wang G C, Zhao D, et al. Research on a novel parallel spoke piezoelectric 6-DOF heavy force/ torque sensor[J]. *Mechanical Systems and Signal Processing*, 2013, 36(1): 152-167

[9] Li Y J, Yang C, Wang G C, et al. Research on the parallel load sharing principle of a novel self-decoupled piezoelectric six-dimensional force sensor[J]. *ISA Transactions*, 2017, 70: 447-457

[10] Hirosea K, Dokia H, Kondoa A. Dynamic analysis and motion measurement of ski turns using inertial and force sensors[J]. *Procedia Engineering*, 2013, 60: 355-360

[11] Yuan C, Luo L P, Yuan Q, et al. Development and evaluation of a compact 6-axis force/moment sensor with a serial structure for the humanoid robot foot[J]. *Measurement*, 2015, 70: 110-122

[12] Sun Y J, Liu Y W, Zou T, et al. Design and optimization of a novel six-axis force/torque sensor for space robot [J]. *Measurement*, 2015, 65: 135-148

[13] Chen D F, Song A G, Li A. Design and calibration of a six-axis force/torque sensor with large measurement range used for the space manipulator [J]. *Procedia Engineering*, 2015, 99: 1164-1170

[14] Zhao Y Z, Zhang C F, Zhang D, et al. Mathematical model and calibration experiment of a large measurement range flexible joints 6-UPUR six-axis force sensor [J]. *Sensors*, 2016, 16(8): 1271

[15] Wang Z J, Yao J T, Xu Y D, et al. Hyperstatic analysis of a fully pre-stressed six-axis force/torque sensor [J]. *Mechanism and Machine Theory*, 2012, 57: 84-94

[16] Murray R M, Li Z X, Sastry S S. A Mathematical Introduction to Robotic Manipulation [M]. Boca Raton: CRC Press, 1994

[17] Diao X M, Ma O. A method of verifying force-closure condition for general cable manipulators with seven cables [J]. *Mechanism and Machine Theory*, 2007, 42: 1563-1576

[18] Pham C B, Yeo S H, Yang G L, et al. Force-closure workspace analysis of cable-driven parallel mechanisms [J]. *Mechanism and Machine Theory*, 2006, 41(1): 53-69

[19] Shi H M, Huang Q B. Mechanical Vibration System-Analysis Test Modeling Countermeasure [M]. Wuhan: Huazhong University of Science and Technology press, 2013 (In Chinese)

[20] Wang Z J, Li Z X, He J, et al. Optimal design and experiment research of a fully pre-stressed six-axis force/torque sensor [J]. *Measurement*, 2013, 46: 2013-2021

Wang Zhijun, born in 1983. He received his B. S. and Ph. D degrees in mechanical-electronic engineering from Yanshan University in 2006 and 2012 respectively. His research interests include the robotic mechanism, six-axis force sensor and robot control technology.